Harrison, R. A., & Lachmann, P. J. (1980) *Mol. Immunol. 17*, 9.
Hürlein, D., Fietzek, P. P., Wachter, E., Lapiere, C. M., & Kühn, K. (1979) *Eur. J. Biochem. 99*, 31.
Ji, T. H. (1983) *Methods Enzymol. 91*, 580.
Johny, K. V., Dasgupta, M. K., Singh, B., & Dosseter, J. B. (1980) *Clin. Exp. Immunol. 40*, 459.
Kühn, K. (1982) in *Immunochemistry of the Extracellular Matrix* (Furthmayr, H., Ed.) Vol. 1, p 1, CRC Press, Boca Raton, Fl.
Lachmann, P. J. (1962) *Immunology 5*, 687.
Lachmann, P. J. (1967) *Adv. Immunol. 6*, 480.
Lachmann, P. J., & Coombs, R. R. A. (1965) in *Complement, Ciba Foundation Symposium* (Walstenholme, G. E. W., & Knight, J., Eds.) p 242, Little, Brown and Co., Boston, Ma.
Lachmann, P. J., & Müller-Eberhard, H. J. (1968) *J. Immunol. 100*, 691.
Laemmli, U. K. (1971) *Nature (London) 227*, 680.
Linscott, W. D., Ranken, R., & Triglia, R. P. (1978) *J. Immunol. 121*, 658.
Mauca, R., Gigliorini, P., Bombardieri, S., & Celada, R. (1980) *Clin. Immunol. Immunopathol. 16*, 131.
Miller, R. L., & Udenfriend, S. (1970) *Arch. Biochem. Biophys. 139*, 104.
Nagasawa, S., & Stroud, R. M. (1977) *Immunochemistry 14*, 749.
Odermatt, E., Risteli, J., Van Delden, V., & Timpl, R. (1983) *Biochem. J. 211*, 295.
Pangburn, M. K., Schreiber, R. D., & Müller-Eberhard, H. J. (1977) *J. Exp. Med. 146*, 257.
Rauterberg, J., Timpl, R., & Furthmayr, H. (1972) *Eur. J. Biochem. 27*, 231.
Reid, K. B. M. (1974) *Biochem. J. 141*, 189.
Reid, K. B. M. (1976) *Biochem. J. 155*, 5.
Reid, K. B., Gagnon, J., & Frampton, J. (1982) *Biochem. J. 203*, 559.
Shinokomaki, M., Duance, V. C., & Baily, A. J. (1980) *FEBS Lett. 121*, 51.
Zalut, C., Henzel, W. S., & Harris, H. W. (1980) *J. Biochem. Biophys. Methods 3*, 11.

^{1}H Nuclear Magnetic Resonance Spectroscopic Study of the Polypeptide Toxin I from *Anemonia sulcata*†

Paul R. Gooley, Laszlo Beress, and Raymond S. Norton*

ABSTRACT: High-resolution ^{1}H nuclear magnetic resonance (NMR) spectroscopy at 300 MHz has been used to study the conformation in aqueous solution of the polypeptide toxin I (ATX I) from the sea anemone *Anemonia sulcata*. Resonances from a number of aromatic and methyl groups have been assigned, in many cases to specific amino acid residues in the sequence. Unusual splitting patterns due to virtual coupling are observed for the aromatic protons of one Trp residue and γ-CH_3 of one Thr residue. ATX I appears to be a flexible molecule but possesses a stable, nonrandom tertiary structure. The latter is characterized by a hydrophobic region encompassing Trp-23 and -31 and several aliphatic residues. A limited region of the molecule coexists in two equally populated structural forms, which are detected by splitting of the methyl resonances from Met-18 and a Thr residue. The aromatic rings of Phe-25 and Tyr-42 are not involved in strong interactions with other residues. The pH and temperature dependencies of the spectrum have been analyzed. pK_a values are obtained for Gly-1 (8.3), Lys-7 and -45 (11.2), Glu-35 (4.1), Tyr-42 (10.4), and one of the two remaining carboxylates, tentatively assigned to Asp-9. Protonation of the latter, at around pH 3, is accompanied by an extensive conformational change.

Sea anemones contain a number of polypeptides and proteins which they use for the capture of prey and for defense. These molecules display a wide variety of biological activities, ranging from cardiostimulants, cardiotoxins, and neurotoxins to hemolysins and protease inhibitors (Beress, 1978, 1982; Norton et al., 1978; Alsen, 1983).

Of particular interest are a series of homologous polypeptides of molecular weight about 5000, isolated from the anemones *Anthopleura xanthogrammica*, *A. elegantissima*, and *Anemonia sulcata*. These molecules exert potent effects on the mammalian heart and on mammalian and crustacean nerves, apparently by binding to the sodium channels of these tissues in such a way as to delay the inactivation of this channel and prolong the action potential (Romey et al., 1976; Bergman et al., 1976; Kodama et al., 1981). This activity has been the subject of intensive investigation, but our knowledge of the electrophysiological properties of these molecules is not matched by an understanding of the structural basis for their observed activities. One of these polypeptides, anthopleurin-A, has been studied by laser Raman, circular dichroism, and fluorescence spectroscopy (Ishizaki et al., 1979), as well as by natural-abundance ^{13}C NMR[1] spectroscopy (Norton & Norton, 1979; Norton et al., 1982). These studies showed that anthopleurin-A is a globular protein containing numerous β-bends and some β-pleated sheet regions and provided limited information on the environments of several amino acid side chains. A second member of this series, *Anemonia sulcata* toxin II (ATX II), has been studied by laser Raman spec-

† From the School of Biochemistry, University of New South Wales, Kensington NSW 2033, Australia (P.R.G. and R.S.N.), and the Department of Toxicology, University of Kiel, D-2300 Kiel 1, Federal Republic of Germany (L.B.). *Received November 10, 1983.* This work was supported in part by grants from the Australian Research Grants Scheme and the Deutsche Forschungsgemeinschaft (Grant BE 55418).

[1] Abbreviations: ATX I, *Anemonia sulcata* toxin I; ATX II, *Anemonia sulcata* toxin II; NMR, nuclear magnetic resonance; DSS, sodium 4,4-dimethyl-4-silapentane-1-sulfonate.

0006-2960/84/0423-2144$01.50/0 © 1984 American Chemical Society

troscopy (Prescott et al., 1976). It was concluded that ATX II contains disordered structures, but not α-helical structures or β-structures, in marked contrast to the findings for anthopleurin-A. However, a natural-abundance ^{13}C NMR study of ATX II (Norton et al., 1980) indicated that the overall conformations of ATX II and anthopleurin-A were indeed similar.

The above studies have provided a limited, qualitative view of the structures of two members of this homologous series. However, a more detailed knowledge of the conformation and dynamics of these molecules is required before their effects on excitable tissues can be interpreted in structural terms. Toward this end, we have carried out a ^{1}H NMR study of *Anemonia sulcata* toxin I (ATX I). This polypeptide, first isolated by Beress et al. (1975a,b), consists of 46 amino acids of known sequence (Wunderer & Eulitz, 1978). It contains three disulfide bonds, which are assumed to have the same arrangement as in ATX II (Wunderer, 1978), with which ATX I shares 65% homology (Wunderer & Eulitz, 1978). The results of our ^{1}H NMR studies of ATX I are presented in this paper.

Materials and Methods

Materials. ATX I was isolated from the sea anemone *Anemonia sulcata* as described previously (Beress et al., 1975a,b). ^2H_2O (>99.75% ^{2}H) was obtained from the Australian Atomic Energy Commission, Lucas Heights, NSW, and ^{2}HCl and NaO^{2}H were from Merck Sharp & Dohme, Montreal. Sephadex G-10 was purchased from Pharmacia Fine Chemicals and Spectra/Por 6 dialysis tubing (molecular weight cutoff 1000) from Spectrum Medical Industries, Los Angeles.

Amino Acid Analysis. Acid hydrolyses were carried out in redistilled 6 M HCl in vacuo at 110 °C for 24 h (Crestfield et al., 1963). To prevent the destruction of Tyr during hydrolysis, 0.1% phenol was added to the 6 M HCl (Sanger & Thompson, 1963). Hydrolysates were dried in vacuo in a clean desiccator over fresh NaOH.

Amino acid analysis was then carried out on a Beckman 121M analyzer. The system consisted of two columns, 47 × 0.28 cm and 4 × 0.28 cm, filled with Beckman W2 resin (10% cross-linked sulfonated polystyrene, 10 ± 2 μm bead size) and run with a flow rate of 15 mL/h. Data reduction was performed by an Autolab System AA integrator, calibrated with a standard amino acid mixture (Pierce Chemicals) run at 10 nmol concentration. Internal standards of norleucine and 2-amino-3-guanidinopropionic acid (Pierce Chemicals) were added to each sample.

NMR Spectroscopy. ^{1}H NMR spectra were recorded at 300.07 MHz on a Bruker CXP-300 spectrometer operating in the pulsed Fourier transform mode with quadrature detection; 5-mm o.d. spinning sample tubes (Wilmad Glass Co., 527-PP grade) were used, and the probe temperature was maintained with a Bruker B-VT 1000 variable temperature unit. Typical spectral accumulation parameters were the following: sweep width 3816 Hz, 8192 addresses, 90° radio-frequency pulses (6.5–7.5 μs duration), 2.0 s recycle time, 500–2000 accumulations, probe temperature 27 °C. Resolution enhancement was effected by means of a Lorentzian–Guassian transformation (Ernst, 1966). Chemical shifts were measured digitally, with 1,4-dioxane, at 3.751 ppm downfield from DSS, as internal standard. Spectral simulations were carried out with the PANIC program on an Aspect 2000 computer.

Samples of ATX I were lyophilized at least twice from ^2H_2O before being dissolved in ^2H_2O at concentrations of 1–2 mM.

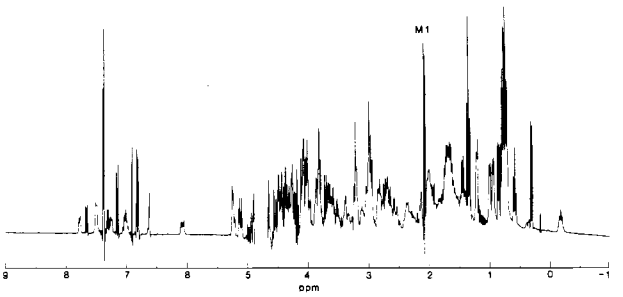

FIGURE 1: 300-MHz ^{1}H NMR spectrum of 2 mM ATX I in ^2H_2O, pH 6.8, at 27 °C. A total of 2240 transients was acquired by using a 90° pulse width, recycle time 2 s, sweep width 3816 Hz, and 8192 data points. The time domain was multiplied by a Lorentz–Gauss window function and zero filled to 32768 data points prior to Fourier transformation.

pH values were measured at 22 °C with an Activon Model 101 pH meter and Ingold 6030–02 microelectrode. Reported values are pH meter readings uncorrected for deuterium isotope effects. The pH was adjusted by adding 0.5 M ^{2}HCl or NaO^{2}H and was measured both before and after NMR experiments. pK_a values were obtained by nonlinear, least-squares fits of the observed chemical shifts to the Henderson–Hasselbalch equation for a single ionization, assuming fast exchange between the conjugate acids and conjugate bases. Samples of ATX I were desalted by gel filtration on Sephadex G-10 or by dialysis.

The two-dimensional homonuclear correlated spectrum (COSY) was recorded with the pulse sequence (Aue et al., 1976; Wagner et al., 1981)

$$[90°-t_1-90°-t_2]_n$$

where t_1 and t_2 are the evolution and observation periods, respectively. The measurement was repeated for 512 equidistant values of t_1, from 0.01 to 170.6 ms. To improve signal to noise, 144 transients were accumulated at each t_1 value. The spectral width was 3000 Hz in each dimension, and in f_2 the data block size was 2048 addresses. Quadrature detection was employed in both dimensions, with appropriate phase cycling to select P-type peaks. The water signal was suppressed by gated decoupling for 0.5 s, and a further delay of 1 s was used between transients. Before Fourier transformation, the time domain matrix was multiplied in the t_1 dimension by a phase-shifted (π/32) sine-squared bell function and in t_2 by a phase-shifted (π/32) sine bell function (Wagner et al., 1978) and zero filled to 1024 points in t_1 and 4096 in t_2. The frequency domain spectrum is shown in the absolute value mode, without symmetrization.

Results

Figure 1 shows the complete ^{1}H NMR spectrum of ATX I at pH 6.8 and 27 °C. Around this pH the chemical shifts of all well-resolved resonances are essentially independent of pH. The spectrum contains a number of resonances shifted significantly from their positions in small peptides, indicating that ATX I has a stable, nonrandom conformation in solution. Notwithstanding this, the absence of any resonances from slowly exchanging groups such as peptide NH protons after only two brief (about 30 min) preexchanges with ^2H_2O at room temperature indicates that the structure possesses some flexibility.

To provide a basis for interpretation of this spectrum, the resonances must be assigned to individual side chains. The next two sections describe assignment of the aromatic and methyl regions of the spectrum. This is followed by a description of the effects of pH and temperature on the spectrum.

10
Gly-Ala-Pro/Ala-Cys-Leu-Cys-Lys-Ser-Asp-Gly-
20
Pro-Asn-Thr-Arg-Gly-Asn-Ser-Met-Ser-Gly-
30
Thr-Ile-Trp-Val-Phe-Gly-Cys-Pro-Ser-Gly-
40
Trp-Asn-Asn-Cys-Glu-Gly-Arg-Ala-Ile-Ile-
46
Gly-Tyr-Cys-Cys-Lys-Gln

FIGURE 2: Amino acid sequence of ATX I (Wunderer & Eulitz, 1978).

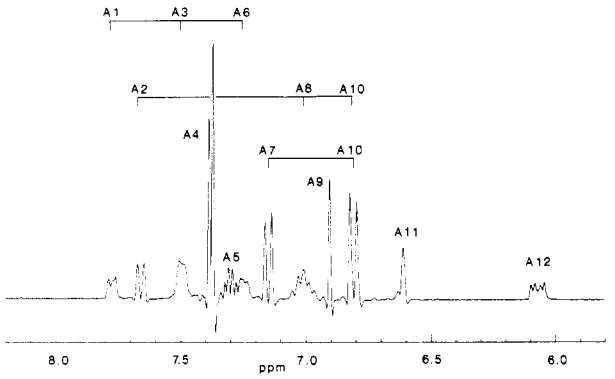

FIGURE 3: Aromatic region of 300-MHz ^1H NMR spectrum of 2 mM ATX I in ^2H_2O, pH 6.8, at 27 °C. Spectral conditions are as described in Figure 1. Peak assignments are described in the text.

To facilitate discussion, the amino acid sequence of ATX I is given in Figure 2.

Aromatic Region. Figure 3 shows the 6–8 ppm region of the spectrum of ATX I, which contains resonances from Trp-23, Trp-31, Phe-25, and Tyr-42, a total of 19 protons. A doublet of doublets near 6.1 ppm (J = 11.5, 4.8 Hz), corresponding to a single aliphatic proton, is also present in this region of the spectrum. Assignments and spin–spin coupling networks were established by two-dimensional homonuclear correlated spectroscopy, in which J couplings between individual protons are manifested as off-diagonal cross-peaks. The aromatic region of this spectrum is shown in Figure 4, with the J connectivities between ortho protons indicated for both Trp residues[2] and for Tyr-45. Assignments are as follows: Trp *a* C(2)H,A9, C(4)H,A6, C(5)H/C(6)H,A3, and C(7)H,A1; Trp *b* C(2)H,A11, C(4)H,A2, C(5)H/C(6)H,A8, and C(7)H,A10; Phe-25 C(2)H to C(6)H,A4 and A5; Tyr-42 C(2,6)H,A7 and C(3,5)H,A10.

Resonances from the two Trp residues are shifted significantly from their positions in small peptides (Bundi & Wüthrich, 1979). The differences are –0.33, –0.39, 0.34/0.26, and 0.28 ppm for C(2)H, C(4)H, C(5)H/C(6)H, and C(7)H, respectively, of Trp *a* and –0.62, 0.02, –0.15/–0.23, and –0.69 ppm for Trp *b*. That these shift perturbations reflect interactions associated with the native conformation of ATX I is shown by the observation that at elevated temperatures (see below) all of the Trp resonances move toward the positions found for peptides. This also confirms the assignments of the four doublets to C(4)H or C(7)H.

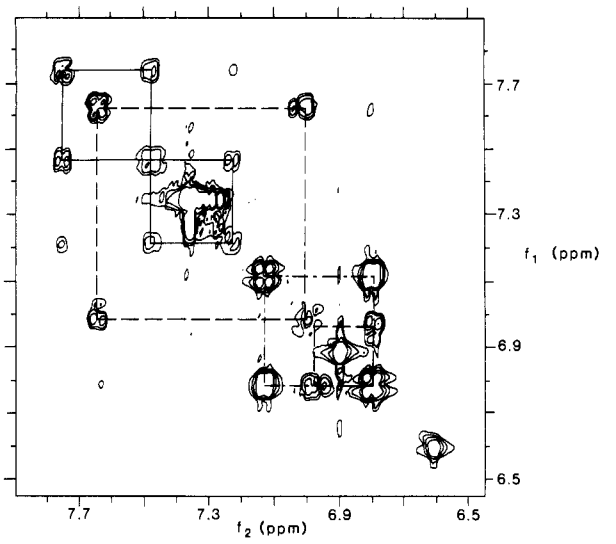

FIGURE 4: Contour plot of the spectral region 6.5–7.9 ppm of a 300-MHz ^1H two-dimensional correlated spectrum from 3 mM ATX I in ^2H_2O, pH 4.5, at 27 °C. Digital resolution in f_1 is 2.9 Hz/point and in f_2 1.46 Hz/point. The spectrum was recorded in about 31 h. Connectivities between ortho protons are shown for the ring systems of Trp *a* (—), Trp *b* (- - -), and Tyr-45 (· · ·).

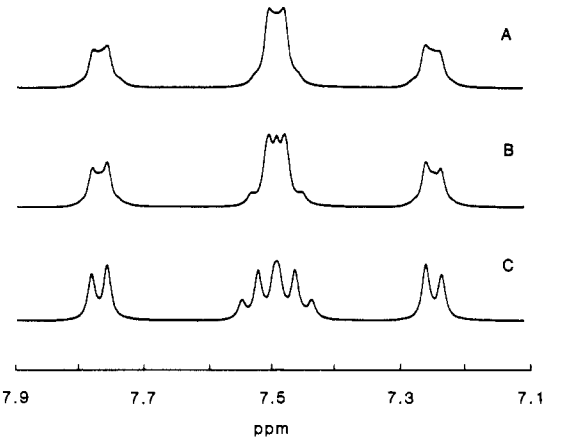

FIGURE 5: Computer simulation of the Trp *a* spin system. (A) $\Delta\delta$ between C(5)H and C(6)H is 2 Hz, which resembles the observed spin system at pH 6.8. (B) $\Delta\delta$ 6 Hz, simulates the Trp ring system at about pH 2.8. (C) $\Delta\delta$ 16 Hz, simulates lower pH values.

The resonances from Trp *a* display an unusual splitting pattern, which is most readily seen for the doublets from C(4)H (A6) and C(7)H (A1). In addition to the expected doublet pattern, each of these protons yields an additional signal of similar height to the two components of the doublet, which is positioned between the other two peaks but displaced slightly toward the C(5)H/C(6)H resonance. The total intensity of each of these "multiplets" corresponds, however, to only a single proton. Because of overlap of the C(5)H and C(6)H resonances, it cannot be ascertained whether they also possess an unusual coupling pattern. Nevertheless, it is clear that the additional components of the C(4)H and C(7)H resonances of Trp *a* are a manifestation of the native conformation, as they disappear reversibly at temperatures above about 55 °C at pH 4.5 or at pH values below 3.3 at 27 °C, under which conditions the resonances revert to simple doublets. At the same time the broad peak arising from C(5)H and C(6)H of Trp *a* also sharpens.

This unusual splitting pattern for Trp *a* appears to be due to virtual coupling (Bovey, 1969), which arises not from the

[2] The J connectivities indicated by boxes in Figure 4 represent ortho couplings. For both Trp rings the H-5 and H-6 resonances overlap with each other, so that cross-peaks due to meta couplings between H-4 and H-6 or H-5 and H-7 cannot be visualized. However, cross-peaks arising from para couplings between H-4 and H-7 *are* visible in Figure 4 for both rings. The existence of cross-peaks due to long-range couplings further confirms our assignments and should prove useful in the analysis of more complex spectra of larger proteins.

Table I: Assignment of Methyl Resonances in the ^{1}H NMR Spectrum of ATX I[a]

resonance[b]	assignment	δ[c]	decoupling position[d]	^3J[e]
M1	Met-18 ε-CH_3	2.059, 2.077 (2.11)		
M2	Ala-3 β-CH_3	1.438 (1.38)	5.00 (4.33)	7.3 (7.0)
M3	Ala-38 β-CH_3	1.352 (1.38)	4.08[f] (4.33)	7.1 (7.0)
M4	Ala-2 β-CH_3	1.331 (1.38)	4.40, 4.63[f] (4.33)	7.1 (7.0)
M5	Thr γ-CH_3	1.207 (1.22)	4.32[f] (4.21)	6.1 (6.3)
M6	Leu-5 δ-CH_3	0.990	1.71 (1.63)	5.4 (6.3)
M7		0.932 (0.93, 0.88)		
M8	Ile γ-CH_3	0.849 (0.93)	1.67 (1.88)	6.7 (6.9)
M9	Ile δ-CH_3[g]	0.79[h] (0.87)	1.44, 1.12 (1.46, 1.18)	7.1 (7.0)
M10	Ile γ-CH_3	0.786[h] (0.93)	1.71 (1.88)	7.2 (6.9)
M11	Val-24 γ-CH_3	0.750[h]	1.63 (2.12)	6.9 (6.9)
M15		0.302 (0.95, 0.93)		
M12	Ile γ-CH_3	0.72[h] (0.93)	1.54[f] (1.88)	7.3 (6.9)
M13	Thr γ-CH_3	0.71[h] (1.22)	3.99 (4.21)	6.1 (6.3)
M14	Ile δ-CH_3	0.583 (0.87)	0.80, 1.04[f] (1.46, 1.18)	7.2 (7.0)
M16	unknown	−0.189	1.38[f]	6.8

[a] In ^2H_2O at pH 6.8 and 27 °C, unless otherwise noted. [b] Numbered as in Figure 6, except for M1, which can be seen in Figure 1. [c] Chemical shift in ppm from DSS. Estimated accuracy 0.003 ppm. Values in parentheses are chemical shifts of corresponding protons in small peptides, obtained by subtracting 0.015 ppm from the data of Bundi & Wüthrich (1979) to correct for the difference between the chemical shifts of DSS and TSP at pH 7. [d] In ppm from DSS. Corresponding values in small peptides, corrected as described in footnote *c*, are given in parentheses. [e] Three-bond coupling constant in hertz (mean of at least two values near pH 6.8). Values in parentheses are for small peptides (Bundi & Wüthrich, 1979). [f] Decoupling position at pH 4.5. These methyl resonances show only slight pH dependence between pH 4.5 and pH 6.8 (see Figure 9). [g] Peak probably arises from two Ile δ-CH_3, as shown by integrated intensities and spectral simulation. [h] Chemical shift obtained initially by selective spin decoupling and confirmed by processing with greater resolution enhancement than in Figure 6 and by spectral simulation.

proximity of the resonances of either C(4)H or C(7)H to those of C(5)H and C(6)H but from the proximity of C(5)H and C(6)H to each other. The observed peak pattern can be simulated by using the PANIC program in the Aspect 2000 computer, as shown in Figure 5. This figure also illustrates the exquisite sensitivity of the appearance of the C(4)H and C(7)H peaks to the chemical shift difference between C(5)H and C(6)H. A change of only 4 Hz in the latter alters the appearance of the C(4)H and C(7)H resonances (Figure 5B), while a change of 14 Hz essentially removes the unusual features of the splitting patterns of C(4)H and C(7)H (Figure 5C), as is observed for ATX I at low pH and/or high temperature. This sensitivity might prove useful in estimating the chemical shifts of resonances from C(5)H and C(6)H in spectra where they cannot be observed directly because of peak overlap but where the C(4)H and/or C(7)H resonances are visible and display such unusual splitting patterns. A similar example of virtual coupling was reported recently in ^{1}H NMR spectra of carbohydrates (Brisson & Carver, 1982).

The five aromatic protons of Phe-25 give rise to a four-proton doublet at 7.377 ppm (A4) and a single-proton multiplet at 7.298 ppm (A5), coupled to each other with an apparent value of 4.7 Hz. These resonances have chemical shifts close to the average value of 7.32 ppm reported for Phe in small peptides (Bundi & Wüthrich, 1979), but the pattern of resonances differs markedly from that in Gly-L-Phe at this frequency (spectrum not shown), indicating that the aromatic ring is not undergoing free rotation about its C1–C4 axis. The chemical shifts of A4 and A5 are independent of pH, but as the temperature is increased, A4 becomes a broad singlet, and A5 broadens and moves downfield toward A4.

The aromatic protons of Tyr-42 yield a pair of sharp, two-proton doublets (J = 8.1 Hz) at 6.804 and 7.144 ppm, assigned to C(3,5)H and C(2,6)H, respectively. This pattern is characteristic of a freely rotating phenolic ring, which is also indicated by the lack of temperature dependence of resonances A7 and A10. The chemical shifts and phenolic pK_a (see below) are nearly identical with those of Tyr in small peptides, which further implies that the Tyr-42 ring is exposed to the solvent.

The remaining resonance in the aromatic region of the spectrum is the doublet of doublets, A12, centered at 6.06 ppm.

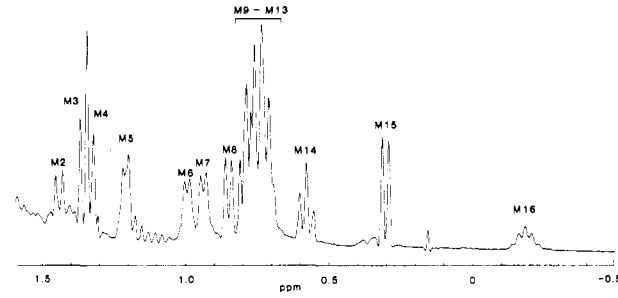

FIGURE 6: Methyl region of 300-MHz ^{1}H NMR spectrum of 2 mM ATX I in ^2H_2O, pH 6.8, at 27 °C. Spectral conditions are the same as in Figure 1. Peak assignments are given in Table I and described in the text. The peak at 0.15 ppm comes from a trace impurity.

This resonance is coupled to peaks at 3.21 and 3.33 ppm. It is assigned to an α-proton, possibly from an aromatic or cystine residue, which presumably owes its significant downfield shift of ≥1.3 ppm (Bundi & Wüthrich, 1979) to the deshielding effects of an aromatic ring or a peptide carbonyl.

Methyl Region. Figure 6 shows an expanded view of the spectrum of ATX I between −0.5 and 1.5 ppm. This region is expected to contain resonances from the methyl groups of three Ala at positions 2, 3, and 38, two Thr at positions 13 and 21, three Ile at positions 22, 39, and 40, Leu-5, and Val-24, a total of 15 methyls. The ε-methyl of Met-18 resonates outside this region at 2.07 ppm (peak M1) and will be considered later. Assignment of the methyl resonances relies heavily on the results of homonuclear spin-decoupling experiments, carried out at pH 2.5, 4.5, and 6.8, and a two-dimensional homonuclear correlated spectrum at pH 4.5.

The doublets M2 to M5 have chemical shifts close to those of Ala β-CH_3 and Thr γ-CH_3 in small peptides and are coupled to resonances between 4 and 5 ppm, where Ala α-CH and Thr β-CH peaks are expected to occur (Table I). As peaks M2, M3, and M4 have coupling constants of 7.0–7.3 Hz, typical of Ala β-CH_3 resonances (Campbell et al., 1975; Bundi & Wüthrich, 1979), they are assigned to the three Ala β-CH_3 groups of ATX I. Peak M5 has a coupling constant of 6.1 Hz, consistent with its assignment to one of the two Thr γ-CH_3 moieties.

The Ala β-CH_3 resonances can be specifically assigned as a consequence of the heterogeneity at position 3 in the sequence (Figure 2). In the sample used here, amino acid analysis and limited sequence analysis using the Edman method show that two-thirds of the material has Ala at position 3 and the remaining one-third Pro. Integration of fully relaxed spectra of ATX I shows that the Ala β-CH_3 resonance M2 has an intensity about 60% that of other resolved methyl resonances. On this basis, M2 is assigned to Ala-3.

Peak M4 integrates for a single methyl group but can be decoupled at two positions in the Ala α-CH region. This can be rationalized if M4 is a composite resonance arising from β-CH_3 of Ala-2 in the two forms of ATX I having Ala or Pro at position 3. Confirmation of this assignment comes from spectra processed so as to give greater peak narrowing than shown in Figure 6; under these conditions peak M4 is resolved into two doublets at pH $\leq$3 with relative heights of 64:36, the further downfield doublet having the greater intensity at each pH. As irradiation at 4.40 ppm is more effective in decoupling M4 than that at 4.63 ppm, it is assumed that α-CH of Ala-2 in ATX I (Ala-3) resonates at 4.40 ppm, while in ATX I (Pro-3) it is at 4.63 ppm. This is consistent with data for peptides (Kopple & Go, 1976; Bundi & Wüthrich, 1979), which show that substitution of Ala by Pro following Val or Gly residues shifts the Val and Gly α-CH resonances downfield by approximately 0.2 ppm.

The remaining β-CH_3 resonance, M3, is assigned by elimination to Ala-38. This integrates for a single methyl group and is decoupled at only one frequency. It shows a greater pH dependence than the other two Ala β-CH_3 resonances, which, as discussed below, is consistent with its assignment.

Peak M5, assigned to one of the Thr γ-CH_3 groups, shows an unusual coupling pattern similar to that observed for the resonances from C(4)H and C(7)H of Trp *a*. At pH >4 there is an additional resonance of similar height to that of the two components of the doublet, located midway between them. This central peak disappears reversibly, leaving a simple doublet with an unchanged coupling constant, at temperatures above about 50 °C at pH 4.5 or at pH values below 3.3 at 27 °C. Thus, not only is the appearance of this additional component similar to those of the Trp resonances but so also are the conditions of pH and temperature under which it is observed. This appears to be another example of virtual coupling, arising here from the proximity of the α-CH and β-CH resonances. Spectral simulation indicates that the chemical shift difference between the α- and β-resonances must be about 2 Hz.

The γ-CH_3 resonance from the second Thr shows even more unusual behavior. The two-dimensional homonuclear correlated spectrum at pH 4.5 shows that peak M13, at 0.71 ppm, is coupled to a resonance at 3.99 ppm, close to the expected position for Thr β-CH (Table I). Nevertheless, irradiation at 3.99 ppm does not collapse peak M13 from a doublet to a singlet, as expected for a Thr γ-CH_3, but from an apparent triplet to a doublet. The latter behavior is consistent with that of an Ile δ-CH_3 resonance. However, two factors militate against such an assignment. First, the position of the coupled resonance, 3.99 ppm, would require a downfield shift of more than 2.5 ppm for an Ile γ-CH, relative to its position in small peptides (Table I). A shift of this magnitude would be difficult to account for, particularly in view of the fact that the chemical shift of peak M13 is close to that of Ile δ-CH_3 in small peptides. Second, the coupling constant for M13, 6.1 Hz (Table I), is unusually small for an Ile δ-CH_3 (although it is consistent with Thr γ-CH_3). While neither of these factors alone provides sufficient grounds for rejecting the assignment to Ile δ-CH_3, they motivate a closer investigation of this resonance.

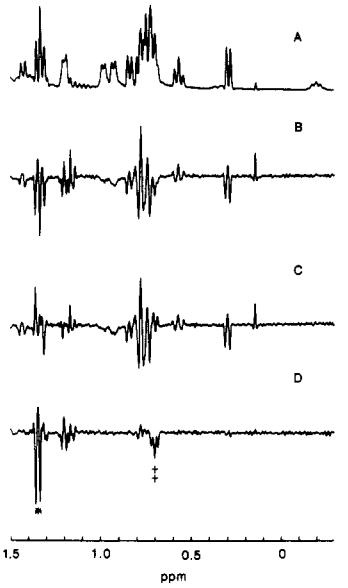

FIGURE 7: Assignment of γ-CH_3 (peak M13) as a pair of overlapping doublets. (A) Normal spectrum of ATX I, pH 6.8, at 27 °C. Spectral conditions are as described in Figure 1. (B) Spin-echo spectrum (90°–t_1–180°–t_1–acquire) with off-resonance decoupling. Irradiation was on at all times except during acquisition; 3904 transients were accumulated with t_1 = 82 ms. Other spectral conditions were the same as (A). (C) Same as (B), but with decoupling at 3.98 ppm. (D) Difference spectrum between (B) and (C). Note that resonances of Thr-21 (‡) are in the same phase as the doublet of Ala-38 (asterisk), indicating that the resonance from Thr-21 consists of overlapping doublets.

Spectra B–D of Figure 7 show the results of a spin-echo double resonance experiment (Campbell & Dobson, 1975) designed to establish whether or not peak M13 was a genuine triplet. The phase of a resonance in a spin-echo spectrum depends on its multiplicity during the evolution period $1/J$, with singlets and triplets being positive and doublets inverted (Figure 7B). Selective irradiation during $1/J$ alters the multiplicity and hence the phase of the signal, but as the irradiation is not applied during data acquisition, the observed multiplicity is not altered. Subtraction of the decoupled spectrum from the unperturbed spectrum therefore gives a difference spectrum consisting of peaks coupled to the irradiated resonance but with intensities twice those of the original resonance and having their original phase. In Figure 7C irradiation was applied during $1/J$ with sufficient power to decouple peaks M3 (Ala-38 β-CH_3) and M13. The difference spectrum, Figure 7D, shows the expected negative doublet from M3 and a negative "triplet" from M13. The phase of the M13 triplet suggests that it is really a superposition of two doublets, each coupled to 4.0 ppm. The simplest explanation of this observation is that peak M13 arises from a Thr γ-CH_3 resonance split into two components of equal intensity and about 6 Hz apart. Such a splitting may arise as a result of restricted rotation about the C^{α}–C^{β} bond, perhaps due to an interaction such as hydrogen bonding of the Thr β-hydroxyl. As both doublets are decoupled by irradiation at 4.0 ppm, it may be concluded that the chemical shifts of the β-CH resonances are relatively close to one another.

Further support for the above interpretation comes from an examination of the temperature dependence of the spectrum at pH 3.2. As the temperature is raised, M13 moves downfield toward the expected position for a Thr γ-CH_3 resonance, assumes the appearance of a doublet, and remains coupled to

a peak near 4.0 ppm. At 67 °C the resonance (now at 0.8 ppm) is still a triplet. At 82 °C it is resolved at 0.99 ppm but is broad. By 87 °C it has moved to 1.025 ppm and is a clear doublet, which can be collapsed to a singlet by decoupling at 4.05 ppm.

A tentative assignment of this resonance can be made by comparison with data from the homologous polypeptide anthopleurin-A (Norton et al., 1978). Of the two Thr residues in ATX I, only Thr-21 is conserved in anthopleurin-A, although the latter has two additional Thr residues at positions 17 and 42. However, the spectrum of anthopleurin-A contains a resolved resonance at 0.36 ppm which has the appearance of a distorted triplet but is coupled to 3.85 ppm (P. R. Gooley and R. S. Norton, unpublished results). It is likely that this arises from a Thr γ-CH_3 group with the same unusual behavior as peak M13 and, as their chemical shifts are similar, that both peaks arise from Thr-21. If this is the case, the local interactions responsible for the unusual appearance of these resonances must be conserved from ATX I to anthopleurin-A. Furthermore, peak M5 would then, by elimination, be assigned to γ-CH_3 of Thr-13.

Of the remaining seven doublets in the methyl region, five (M8, M10–M12, and M15) have $J(CH–CH_3) \geq 6.8$ Hz, indicating that they arise from γ-CH_3 groups of Val or Ile (Table I). Peaks M11 and M15 are simultaneously decoupled by irradiation at 1.63 ppm and are assigned to the γ-CH_3 groups of Val-24. The other three are decoupled separately by irradiation in the region 1.5–1.7 ppm, consistent with their assignment to the γ-CH_3 groups of Ile-22, -39, and -40. As noted above, Ala β-CH_3 doublets also have coupling constants around 7 Hz, but the clear separation between the range of decoupling frequencies for those resonances (4–5 ppm) and that of the five doublets considered here (1.5–1.7 ppm) provides strong support for our assignments.

The other two doublets in this region, peaks M6 and M7, share coupling constants of only 5.4 Hz (Table I), suggesting that they come from the two δ-CH_3 groups of Leu-5 (Campbell et al., 1975; Bundi & Wüthrich, 1979). This is confirmed by the observation that they are simultaneously decoupled by irradiation at 1.71 ppm.

It remains to assign the three Ile δ-CH_3 resonances, which are expected to be triplets due to their coupling to the two γ-CH protons. Peak M14 clearly arises from one Ile δ-CH_3, coupled to γ-CH protons at 0.80 and 1.04 ppm. The other two Ile δ-CH_3 groups give rise to the triplet M9, which forms part of the envelope M9–M13 (Figure 6). Decoupling difference spectra indicate that irradiation at either 1.12 or 1.44 ppm converts peak M9 from a triplet to a doublet. These connectivities were confirmed by recording a modified spin-echo spectrum using the pulse sequence [90°–t_1–180°–t_1–90°–t_2–90°–acquire], where t_1 = 70 ms [(1/(2J)] and t_2 = 60 ms (Lecomte et al., 1982). This sequence suppresses methyl doublets, thus permitting clearer observation of triplets. Peak M9 is a prominent triplet in such spectra but is significantly suppressed when irradiation is applied continuously at either 1.12 or 1.44 ppm, thus confirming the above interpretation. That two Ile residues contribute to peak M9 is shown by partial integration of the region M9–M13 and by spectral simulation. The δ-CH_3 and γ-CH_2 resonances of these Ile residues have chemical shifts nearly identical with those in small peptides (Table I).

The remaining well-resolved resonance in the methyl region is peak M16, which appears to be a quintet with a coupling constant of 6.8 Hz. Its integrated intensity corresponds to approximately two protons. At pH <3, it splits reversibly into two broad components of equal intensity, one of which moves further upfield to −0.34 ppm (pH 1.3) while the other remains at −0.2 ppm. At high temperature (pH 4.5), M16 moves downfield and broadens, indicating that it is in intermediate exchange (Dwek, 1973) with its resonance(s) in heat-denatured ATX I. The assignment of peak M16 has not been established.

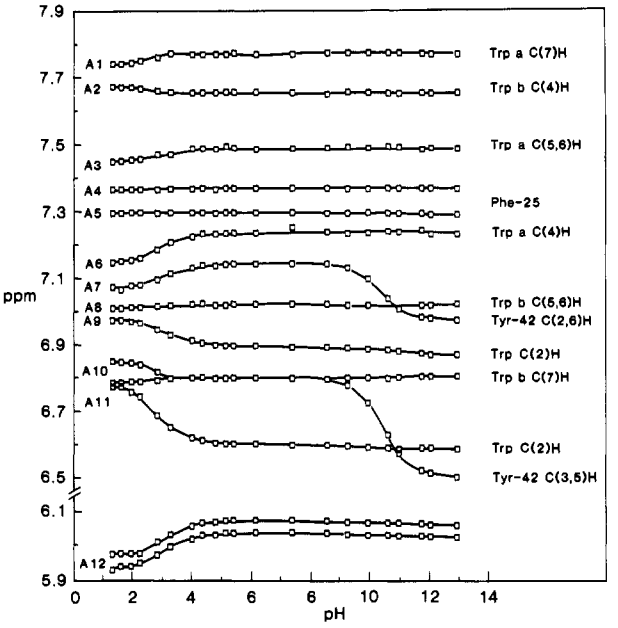

FIGURE 8: pH dependence of the chemical shifts of aromatic proton resonances of ATX I in ^2H_2O at 27 °C. Protein concentrations varied but were typically 1 mM. Spectral conditions were as described in Figure 1, except that 2000 transients were accumulated.

There is also a broad multiplet at 0.35 ppm, just downfield of peak M15 (Figure 6), which is coupled to protons at 1.20 ppm. This resonance moves downfield reversibly at high pH or high temperature but has not yet been assigned. In addition, integration of the envelope M9–M13 gives an intensity of approximately 20 protons, corresponding to six methyl resonances and two extra protons. One of the latter corresponds to a γ-CH of the Ile residue which gives rise to peak M14. The other has not been identified as yet.

Finally, consider peak M1, from ϵ-CH_3 of Met-18. As can be seen in Figure 1 this peak is split into two sharp singlets of equal intensity at 2.059 and 2.077 ppm (Table I). Amino acid analysis of the ATX I sample used in these NMR experiments confirms that only one Met residue is present. Furthermore, the second component is not due to the methyl resonance of acetate, as a small peak due to this impurity can be observed separate from M1*a* and -*b* and its pH titration followed. As in the case of the methyl group which gives rise to peak M13, our interpretation is that there are two separate environments for Met-18 ϵ-CH_3. At pH < 3 and 27 °C the peaks move together and have merged by pH 2.2. At temperatures above 55 °C (pH 4.5) the peaks also merge. In each case the process is reversible. Thus, the dependence of this splitting on temperature and pH resembles those of the appearance of additional components in the resonances of Trp *a* and one of the Thr γ-CH_3 groups (peak M5). The splitting of peak M13 is, however, not collapsed at these values of pH and temperature.

Effects of pH. The pH dependence of the spectrum of ATX I has been examined over the range 1.3–12.9 at 27 °C. In the aromatic region (Figure 8), the resonances of Phe-25 are invariant with pH, while those of Tyr-42 are affected directly by ionization of the phenolic group at high pH and indirectly by protonation of a carboxylate at low pH. The two Trp

Table II: Titration Behavior of Residues in ATX I in ^2H_2O at 27 °C[a]

residue	proton (resonance)	δ_A	$\delta_A - \delta_B$	pK_a (SD)
Tyr-42	C(2,6)H (A7)	7.14	0.17	10.36 (0.11)
		7.07	−0.07	3.2 (0.21)
	C(3,5)H (A10)	6.80	0.29	10.43 (0.13)
		6.79	−0.02	3.1 (0.29)
Trp	C(2)H (A9)	6.97	0.08	3.2 (0.23)
	C(2)H (A11)	6.78	0.18	2.80 (0.15)
Trp *a*	C(4)H (A6)	7.14	−0.09	2.95 (0.19)
unknown	α-CH (A12)[b]	5.96	−0.10	3.1 (0.20)
Leu-5	δ-CH_3 (M6)	0.92	−0.07	2.8 (0.21)
	δ-CH_3 (M7)	0.86	−0.06	2.8 (0.22)
Ala-3	β-CH_3 (M2)	1.46	0.02	2.9 (0.31)
Ala-38	β-CH_3 (M3)	1.26	−0.08	3.0 (0.21)
Ile	δ-CH_3 (M14)	0.70	0.12	3.0 (0.22)
Val-24	γ-CH_3 (M15)	0.33	0.03	2.9 (0.25)
unknown	(M16)[c]	−0.35	−0.15	2.53 (0.19)
Glu-35	γ-CH_2	2.49	0.37	4.09 (0.13)
Lys-7, -45[d]	ε-CH_2	2.98	0.41	11.2 (0.2)
		3.01	0.04	4.21 (0.19)[e]

[a] δ_A and δ_B are limiting chemical shifts at the acidic and basic extremes of the titration to which the pK_a refers. pK_a values were determined from nonlinear least-squares fits to the equation for a single ionization, assuming a slope of 1.0. Standard deviations are given in parentheses. [b] Also moves upfield by 0.015 ppm at high pH. [c] Peak splits into two equal multiplets at pH <3.5. One remains at −0.2 ppm; titration data are for the second multiplet. [d] Overlap prevents determination of separate pK_a values. [e] Data refers to titration of only one Lys ε-CH_2 resonance. The second resonance also shifts slightly at low pH.

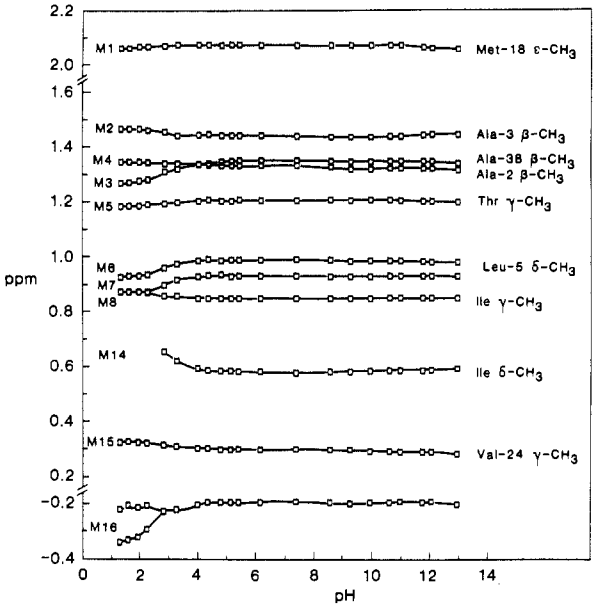

FIGURE 9: pH dependence of the chemical shifts of methyl proton resonances of ATX I in ^2H_2O at 27 °C. Other conditions as in Figure 8.

residues and peak A12 are also affected by the protonation of carboxylates.

Apparent pK_a values for Tyr-42 and for the carboxylates which affect the aromatic region are given in Table II. The pK_a for the phenolic group of Tyr-42 is very close to that in model peptides, viz., 10.3 in Gly-Gly-Tyr-Ala (Bundi & Wüthrich, 1979) and 10.13 in *N*-methyltyrosinamide (Endo et al., 1981), suggesting that this residue is exposed to solvent.

The pH dependence of well-resolved resonances in the methyl region is shown in Figure 9. Many of these resonances are affected by protonation of one or more carboxylates with pK_a values around 3 (Table II). Peak M16 splits into two broad multiplets below pH 3.5, one of which remains at −0.2 ppm while the other moves even further upfield to −0.35 ppm at pH 1. Peak M4, from Ala-2 β-CH_3, exhibits two inflections, one with pK_a = 3.3 (0.5), δ_A 1.34 and δ_B 1.33, and the other with pK_a = 8.3 (0.4), δ_A 1.33 and δ_B 1.32. The latter must correspond to the N-terminal pK_a.

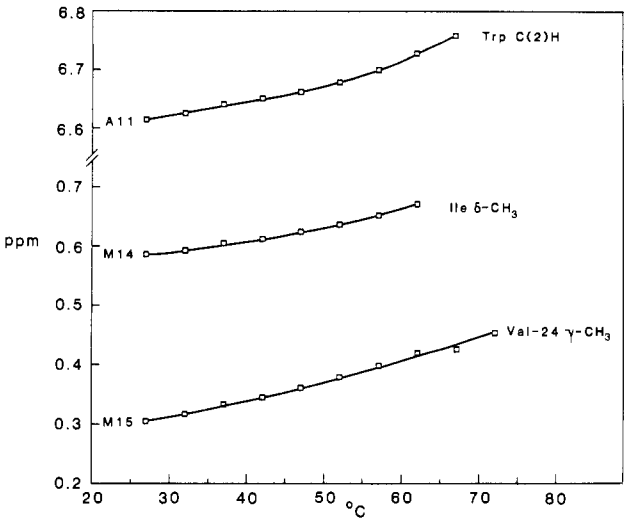

FIGURE 10: Temperature dependence of some resolved resonances of 0.5 mM ATX I in ^2H_2O, pH 4.5. Spectral conditions were as described in Figure 1, except that 1500 transients were accumulated.

The γ-CH_2 resonances of Glu-35, at 2.11 ppm, titrate with pK_a = 4.09 (Table II). Resonances from Lys-7 and Lys-45 yield a multiplet near 3.0 ppm (Figure 1) which titrates at high pH with an average pK_a of 11.2 (Table II). The pattern of peaks in the multiplet changes with pH, indicating that the two Lys residues have slightly different pK_a values, but peak resolution is not sufficient to allow individual pK_a values to be determined. At low pH, one resonance exhibits a downfield shift of 0.04 ppm, with pK_a = 4.2, while the other moves downfield by a smaller amount.

The δ-CH_2 triplets of Arg-14 and -37 show no high pH shift up to pH 12.1 but move upfield by 0.02 ppm at pH 12.9. At low pH, one resonance moves upfield by 0.03 ppm. The midpoint of this inflection is in the range pH 3–3.5, but the data do not give a satisfactory fit to the equation for a single ionization, suggesting that the change in chemical shift may be due to the effects of more than one nearby ionizable group.

Temperature Dependence. The effects of temperature on the spectrum of ATX I at pH 4.5 were examined over the range 27–72 °C. The behavior of a number of resonances, including those from Trp-23,31, Phe-25, Tyr-42, Thr-13,21, Met-18, and peak M16, has already been described (see above). In general, peaks become sharper at higher temperatures, indicating increased flexibility of side chains, probably also accompanied by a decrease in the correlation time(s) for overall molecular reorientation. As shown in Figure 10, shifted resonances move in the direction of their random coil positions at high temperature, but even at 72 °C, the transition to a heat-denatured protein is far from complete. The highly shifted peaks A12 and M16 shift and broaden above 55 °C, indicating that they are in intermediate exchange with their resonances in heat-denatured ATX I.

Discussion

In this paper we have assigned a large number of resonances in the ^1H NMR spectrum of ATX I and examined the effects of pH and temperature on the spectrum. The overall sharpness of the spectrum, together with the observation of a number of resonances at chemical shifts near their values in small peptides, suggests that ATX I has an open, flexible structure.

This is further supported by the absence from the spectrum of resonances due to slowly exchanging peptide NH protons. However, no doubt due partly to the presence of three disulfide bonds in the molecule, there are a number of strong interactions among residues distant from each other in the amino acid sequence, manifested by the presence of many perturbed resonances in the spectrum. Ionic interactions are also important in maintaining the native structure, as protonation of a carboxylate around pH 3 causes extensive local conformational changes. In the following discussion, the environments of individual residues will be summarized, and then the structural features which may be inferred from our data will be described.

Of the four aromatic residues in ATX I, Phe-25 and Tyr-42 appear to be largely solvent exposed and not involved in significant interactions with other residues, while Trp-23 and -31 interact with each other. The environment of Phe-25 is inferred from observations that its chemical shifts are close to those in small peptides and show no pH dependence. At high temperature, some changes are observed in its splitting pattern, indicating an increase in freedom of motion, probably about its C1–C4 axis. The aromatic protons of Tyr-42 yield a pair of sharp doublets, characteristic of a freely rotating phenolic ring. Consistent with this, the resonances are independent of temperature over the range examined. Furthermore, the pK_a of the phenolic group is essentially identical with those of Tyr in small peptides. The aromatic resonances of Tyr-42 are slightly perturbed by the conformational transition at pH 3, but the C(2,6)H doublet is affected to a greater extent than the C(3,5)H, suggesting that these shifts result from movement of the peptide backbone.

Resonances from Trp-23 and-31 are shifted significantly from their positions in small peptides, by up to 0.7 ppm. The most likely causes of such perturbations are ring current shifts from other aromatic rings (Perkins & Wüthrich, 1979; Perkins & Dwek, 1980). Shifts due to the anisotropy of peptide carbonyls are probably not significant for these side chains (Perkins & Dwek, 1980). As the aromatic rings of Phe-25 and Tyr-42 do not interact with other residues, the perturbations of the Trp aromatic resonances must arise from their mutual interaction. When the magnitudes and directions of the observed shifts are taken into account, the indole rings must be oriented such that C(2)H and C(4)H of ring *a* are in the shielding cone of ring *b*, with C(5)H–C(7)H in its deshielding cone, while in ring *b* C(2)H and C(7)H are closest to ring *a* and C(4)H is positioned in an isoshielding zone.

All of the Trp aromatic resonances are affected by the conformational transition which occurs around pH 3. The largest change occurs for peak A11 [Trp C(2)H], which moves downfield by 0.18 ppm. Most of the Trp resonances move in the direction of their random coil chemical shifts at low pH, but C(4)H of Trp *a* moves in the opposite direction, even further upfield. Thus, while some of the interactions in native ATX I are disrupted at low pH, the acid-denatured form is by no means a random coil structure.

Considering now the methyl-containing residues, the β-CH_3 and α-CH resonances from all three Ala residues have been specifically assigned. The sequence heterogeneity at position 3 (Figure 2) is reflected in both a reduced intensity for the Ala-3 β-CH_3 resonance and in chemical shift heterogeneity for the Ala-2 α-CH and β-CH_3 resonances. The Ala-38 β-CH_3 resonance undergoes a much larger shift at low pH than the others, the significance of which will be discussed.

The γ-CH_3 resonances of the two Thr residues both display unexpected splitting patterns. That of Thr-13 (peak M5) is affected by virtual coupling, a manifestation of the near overlap of its α-CH and β-CH resonances. Effects of virtual coupling are also observed for the C(4)H and C(7)H resonances of Trp *a*, in this case due to overlap of its C(5)H and C(6)H resonances. The γ-CH_3 resonance of the second Thr, Thr-21, is split into two equal doublets separated by about 6 Hz, suggesting that this residue occurs in two different environments, which are in slow exchange with one another. This may reflect restricted rotation about the C^α–C^β bond in Thr-21, possibly due to hydrogen bonding of the β-hydroxyl. A similar splitting into two equal components in slow exchange is observed for Met-18 ϵ-CH_3. Given the proximity of these two residues in the ATX I sequence, it is tempting to ascribe both observations to a region of local conformational heterogeneity in the molecule. However, although the chemical shift differences between the two components are very similar (6 Hz for Thr-21 γ-CH_3 and 5 Hz for Met-18 ϵ-CH_3), the Met-18 resonance collapses to a sharp singlet above 55 °C (pH 4.5), while the Thr-21 resonance does not collapse until >70 °C. Thus, although the effects may arise from the same conformational feature, the Met-18 ϵ-CH_3 group is clearly able to free itself from the structural constraints so imposed more readily than the Thr-21 γ-CH_3. It should be noted that the latter resonance is shifted upfield by 0.5 ppm from its position in small peptides, indicating its proximity to an aromatic ring.

Ring current shifts (0.2 and 0.6 ppm) are observed for the two γ-CH_3 resonances of Val-24. These are no doubt due to interactions of these methyls with Trp-23 and Phe-25, although, because of the spatial proximity of Trp-23 and Trp-31, some contribution from the latter cannot be discounted. The Ile δ-CH_3 triplet M14 is also shifted upfield by 0.3 ppm. More dramatic ring current shifts are experienced by peak M16 and the broad peak just downfield from M15. The two protons buried under the methyl peaks at 0.7–0.8 ppm presumably also experience ring current shifts. Further work is required to assign these resonances.

The ionization behavior of most titratable residues in ATX I has been characterized, with pK_a values being determined for Glu-35, Gly-1, Tyr-42, Lys-7, and Lys-45. The guanidinium moieties of Arg-14 and -37 have pK_a > 14. The titration of a carboxylate with pK_a = 3 is detected through its effects on a number of other residues in the molecule. This titration must correspond to γ-COOH of Asp-9, α-COOH of Gln-46, or both. We would expect the C-terminus of ATX I to have a pK_a near 3.5, as its C-terminal sequence is identical with those of the homologous polypeptides ATX II and anthopleurin-A (see introduction), for which ^{13}C NMR studies (Norton et al., 1980, 1982) have yielded C-terminal pK_a values of 3.5. Extending this analogy further, we note that in ATX II and anthopleurin-A, protonation of the C-terminus is not accompanied by any changes in ^{13}C chemical shifts from other residues, which would be consistent with the lack of effect of any group with pK_a = 3.5 on resolved ^{1}H resonances in the spectrum of ATX I and would suggest that the group whose protonation causes a significant change in the conformation of ATX I is not Gln-46 α-COOH. Thus, although we cannot rule out the possibility that this carboxylate has a pK_a near 3 and that the effects of its titration are masked by those of the other carboxylate, we believe that the conformationally significant carboxylate with pK_a = 3 is Asp-9 γ-COOH.

The nature of the interactions between Asp-9 and other residues which make it so important in maintaining the native conformation of ATX I has not been elucidated. It is noteworthy that Glu-35 interacts with the side chain of either Lys-7 or Lys-45, as shown by the low pH inflection in the chemical

shift of one of their ϵ-CH_2 resonances. This interaction must be fairly weak, as it does not significantly change the pK_a's of either group from their values in peptides (Bundi & Wüthrich, 1979). However, given the existence of a disulfide bond between Cys-6 and Cys-34, Lys-7 is probably the residue involved. Even if the two segments of peptide backbone diverge after this point, it is likely that the side chains of Asp-9 and Arg-37 would be close enough to interact. The lower than normal pK_a for Asp-9 is consistent with its interaction with a postively charged moiety.

Whatever the nature of the interactions Asp-9 is involved in, it is clear that their disruption is accompanied by a significant conformational change. We may divide the residues affected by this change loosely into two categories. In the first are Trp-23 and -31 and Val-24, which are distant in the sequence from Asp-9 or Arg-37. It is likely that these residues form part of a "hydrophobic pocket", which is disrupted at low pH. On the basis of the significant ring current shift for γ-CH_3 of Thr-21, this residue is probably also involved in this region. Because of peak overlap, we cannot follow the pH dependence of this resonance. Other participants are likely to be the Ile residue which gives rise to the ring current shifted peak M14, as well as the residue giving rise to peak M16. Somewhat surprisingly, Phe-25 is not part of this region, and its chemical shifts are absolutely invariant with pH. In the second category we would place residues which are affected because of their proximity in the sequence to Asp-9 or Arg-37, the best example being Ala-38. Leu-5 probably belongs in this category, because both of its δ-CH_3 resonances have chemical shifts essentially identical with those in model peptides, making it unlikely that it is close to an aromatic ring. Changes in the chemical shift and splitting pattern at low pH of peak M5, from Thr-13 γ-CH_3, probably reflect a propagation of these changes along the peptide backbone from Asp-9. It is not clear whether the effects on Tyr-42 also belong in this category, but the fact that the C(2,6)H doublet is affected significantly more than that of C(3,5)H suggests that the effects result from a change involving the peptide backbone.

In summary, ATX I is a flexible molecule, which nevertheless possesses a stable, nonrandom, tertiary structure. This structure is stabilized not only by the three disulfide bonds but also by an interaction involving the carboxylate of Asp-9. An ionic interaction between Glu-35 and Lys-7 does not appear to be critical in maintaining the native conformation. ATX I also contains a region of hydrophobic side chains. Part of this region exhibits conformational heterogeneity, which is reflected by different environments for the side chains of at least two residues. Further work is directed toward characterizing the structure of ATX I in solution by making further resonance assignments and then by probing interproton distances by using both one- and two-dimensional nuclear Overhauser enhancement measurements.

Acknowledgments

We are grateful to Dr. J. W. Blunt (Department of Chemistry, University of Canterbury, Christchurch, New Zealand) for pointing out the origin of virtual coupling effects in our spectra and for assistance with computing, Dr. J. K. Saunders (University of New South Wales NMR Centre) for advice regarding the CXP-300 NMR spectrometer, and R. Mann for amino acid analyses. Thanks are also due to J. Zwick for skillful technical assistance in the preparation of ATX I.

Registry No. ATX I, 89177-43-5.

References

Alsen, C. (1983) *Fed. Proc., Fed. Am. Soc. Exp. Biol. 42*, 101–108.

Aue, W. P., Bartholdi, E., & Ernst, R. R. (1976) *J. Chem. Phys. 64*, 2229–2246.

Beress, L. (1978) in *Drugs and Food from the Sea. Myth or Reality*? (Kaul, P. N., & Sindermann, C. J., Eds.) pp 59–72, University of Oklahoma Press, Norman, OK.

Beress, L. (1982) *Pure Appl. Chem. 54*, 1981–1994.

Beress, L., Beress, R., & Wunderer, G. (1975a) *FEBS Lett. 50*, 311–314.

Beress, L., Beress, R., & Wunderer, G. (1975b) *Toxicon 13*, 359–367.

Bergman, C., Dubois, J. M., Rojas, E., & Rathmayer, W. (1976) *Biochim. Biophys. Acta 455*, 173–184.

Bovey, F. A. (1969) *Nuclear Magnetic Resonance Spectroscopy*, Academic Press, New York.

Brisson, J.-R., & Carver, J. P. (1982) *J. Biol. Chem. 257*, 11207–11209.

Bundi, A., & Wüthrich, K. (1979) *Biopolymers 18*, 285–297.

Campbell, I. D., & Dobson, C. M. (1975) *J. Chem. Soc., Chem. Commun.*, 750–751.

Campbell, I. D., Dobson, C. M., & Williams, R. J. P. (1975) *Proc. R. Soc. London, Ser. A 345*, 23–40.

Crestfield, A. M., Moore, S., & Stein, W. H. (1963) *J. Biol. Chem. 238*, 622–627.

Dwek, R. (1973) *Nuclear Magnetic Resonance in Biochemistry*, Chapter 2, Oxford University Press, London.

Endo, T., Inagaki, F., Hayashi, K., & Miyazawa, T. (1981) *Eur. J. Biochem. 120*, 117–124.

Ernst, R. R. (1966) *Adv. Magn. Reson. 2*, 1–135.

Ishizaki, H., McKay, R. H., Norton, T. R., Yasunobu, K. T., Lee, J., & Tu, A. (1979) *J. Biol. Chem. 254*, 9651–9656.

Kodama, I., Shibata, S., Toyama, J., & Yamada, K. (1981) *Br. J. Pharmacol. 74*, 29–37.

Kopple, K. D., & Go, A. (1976) *Biopolymers 15*, 1701–1715.

Lecomte, J. T. J., De Marco, A., & Llinas, M. (1982) *Biochim. Biophys. Acta 703*, 223–230.

Norton, R. S., & Norton, T. R. (1979) *J. Biol. Chem. 254*, 10220–10226.

Norton, R. S., Zwick, J., & Beress, L. (1980) *Eur. J. Biochem. 113*, 75–83.

Norton, R. S., Norton, T. R., Sleigh, R. W., & Bishop, D. G. (1982) *Arch. Biochem. Biophys. 213*, 87–97.

Norton, T. R., Kashiwagi, M., & Shibata, S. (1978) in *Drugs and Food from the Sea. Myth or Reality*? (Kaul, P. N., & Sindermann, C. J., Eds.) pp 37–50, University of Oklahoma Press, Norman, OK.

Perkins, S. J., & Wüthrich, K. (1979) *Biochim. Biophys. Acta 576*, 409–423.

Perkins, S. J., & Dwek, R. A. (1980) *Biochemistry 19*, 245–258.

Prescott, B., Thomas, G. J., Beress, L., Wunderer, G., & Tu, A. T. (1976) *FEBS Lett. 64*, 144–147.

Romey, G., Abita, J. P., Schweitz, H., Wunderer, G., & Lazdunski, M. (1976) *Proc. Natl. Acad. Sci. U.S.A. 73*, 4055–4059.

Sanger, F., & Thompson, E. O. P. (1963) *Biochim. Biophys. Acta 71*, 468–471.

Wagner, G., Wüthrich, K., & Tschesche, H. (1978) *Eur. J. Biochem. 86*, 67–76.

Wagner, G., Kumar, A., & Wüthrich, K. (1981) *Eur. J. Biochem. 114*, 375–384.

Wunderer, G. (1978) *Hoppe-Seyler's Z. Physiol. Chem. 359*, 1193–1201.

Wunderer, G., & Eulitz, M. (1978) *Eur. J. Biochem. 89*, 11–17.